1 Introduction

The study described in this thesis is focused on developing empirical models of flame dynamics, or the response of a flame to perturbations in velocity and equivalence ratio. The primary rationale towards developing simple, compact models is to predict and control thermoacoustic instabilities in gas turbines and aero-engines without the need of time-intensive computations. This chapter outlines the motivation, objectives, and approach of the investigation into the dynamics of laminar and turbulent flames.

1.1 Motivation

Increased energy demands, coupled with the necessity to reduce environmental impact, have underscored the need for clean energy sources. In 2002, the Department of Energy stated, "Of the next 1000 power plants to be built in the United States, as many as 900 of them are likely to use natural gas turbines." The current Advanced Turbine Systems initiative of the DOE seeks near zero (1-2 ppm) NOx and CO emissions. The current state of the art is approximately 10 ppm (General Electric 7H). To achieve decreased emissions, gas turbines must operate very close to the flame's lean limit of extinction, making the flame prone to thermoacoustic instabilities. Thermoacoustic instabilities are a result of the interaction between the acoustics of the combustor and the unsteady heat release rate of the flame. As seen in Figure 1, the acoustics of the combustor produce an unsteady velocity, u', and equivalence ratio, Φ', input to the flame. This unsteady input results in an unsteady heat release rate, q', which then forces the acoustics. The coupling results in large-scale pressure oscillations that prohibit ultra-lean operation. Thus, means to prevent and control thermo-acoustic instabilities must be devised to further decrease emissions from gas turbines.

Industry currently has no means to predict TA instabilities in the design stage. Designers rely on rules of thumb and then must "design out" instabilities via passive means (i.e. baffles and resonators) and by restricting operating conditions. Since gas

turbines are often used as “peakers”, or only operated during peak power demands, restricting certain operating conditions is particularly unattractive. Although Computational Fluid Dynamics (CFD) models may hold the ability to predict TA instabilities, CFD simulations of reacting flows are still in their infancy. The computational expense of a full-physics model of an entire combustor (likely several weeks on a 32-processor machine) makes CFD unrealizable as an industry tool.

In addition to providing the ability to predict TA instabilities using simple, compact models, ROM will also provide a basis to develop model-based controllers for active combustion control (ACC). The current state of the art in ACC controllers rely on adaptive filters with no a priori knowledge of the plant (i.e. combustor). Model-based controllers have the potential to significantly reduce control time, authority requirements, and improved range of applicability.

To develop design strategies and control algorithms for the suppression of pressure oscillations, physics-based models of thermo-acoustic instabilities are needed. The focus of this study is to develop low-order models of flame dynamics, or the response of the unsteady heat release of the flame to perturbations in velocity.

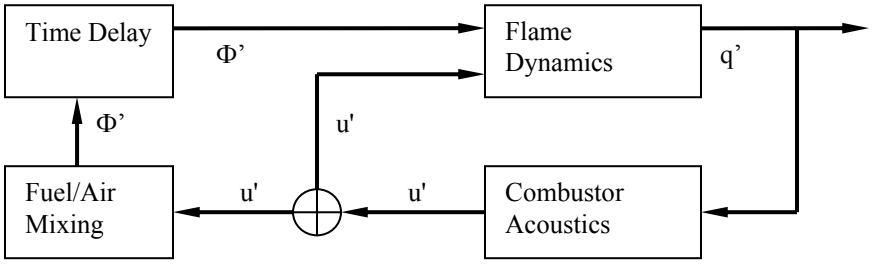

Figure 1.1. System Diagram. System diagram of self-excited thermoacoustic instabilities.

1.2 Objectives

The objective of this study is to develop reduced-order models of flame dynamics. The models will be physics-based, allowing for application in various combustors. Compact, or low-order, models will define the physical processes that govern

thermoacoustic instabilities. Currently, industry is lacking compact models that accurately describe and predict thermoacoustic instabilities. Designers must perform design iterations experimentally, costing time and money. Low-order models allow the designer to run simulations to predict instabilities in minutes, whereas Computational Fluid Dynamics simulations require weeks or months. Also, real-time active control strategies can be based on these compact models to suppress instabilities. By reducing the effect of thermoacoustic instabilities, gas turbines will be able to run at leaner conditions and near-zero NOx and CO emissions can be achieved.

1.3 Background

This section gives background information on topics integral to the study of flame dynamics. Fundamentals of semiconductor lasers, absorption spectroscopy, chemiluminescence, and dynamic systems are discussed.

1.3.1 Semiconductor Lasers. Semiconductor lasers, originally developed for the communications industry, have found widespread use in spectroscopic applications. Room-temperature operation, wavelength tuning, high spectral purity, long-term stability, relative low cost, and compatibility with fiber optic networks allow diode lasers to be useful in a wide range of industrial and laboratory applications [1]. Diode lasers are commercially available in a range of wavelengths from approximately 630 nm to 2200 nm. Thus, Tunable Diode Laser Absorption Spectroscopy (TDLAS) methods are able to access the absorption bands of many species important in combustion flows. Table 1.2 provides a summary of important absorption bands. Diode lasers can be wavelength tuned via injection current and temperature. This allows one to capture the entire absorption feature in order to measure spectroscopic quantities including species concentration, temperature, pressure, and line broadening.

In addition to the many advantages of diode lasers, there are several disadvantages. Diode lasers are exceedingly susceptible to damage from electro-static discharge, so care must be taken when installing and designing the experimental setup.

Also, the beams from diode lasers, especially those of the distributed feedback (DFB) type, are highly diffuse and the divergence is asymmetrical, making collimation a challenge. As with any infrared light, the beams are invisible to the naked eye and a card coated with material that fluoresces in IR light must be used to visualize the beam.

Table 1.2 Relevant Absorption Bands. Absorption Bands of Species in Combustion.

Species	Transition, cm^{-1}
H20	7444.37, 7185.59, 5558.18
CO	4311.96, 4343.81,
O2	13142.58, 13140.57

1.3.2 Absorption Spectroscopy[1]. Quantitative absorption spectroscopy uses the absorption spectra of molecules to determine concentrations, temperatures, and other physical properties. A typical experimental setup is shown in Figure 1.3. A coherent light beam is passed through a beamsplitter to a detector that measures the incident optical power. The remaining light is passed through an absorbing media, then to a second detector. The ratio of the absorbed light to the incident light is the transmittance.

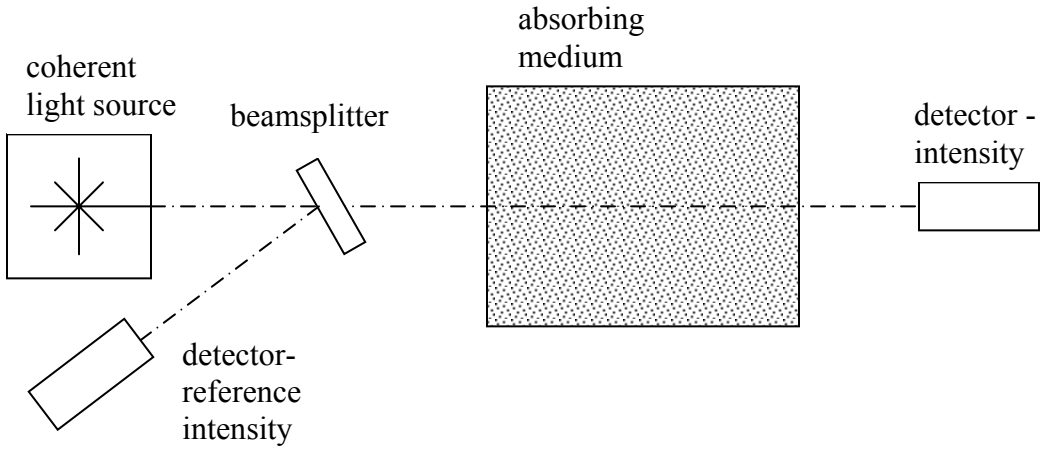

Figure 1.3. Typical Absorption Spectroscopy Experimental Setup.

[1] The theses of Edward R. Furlong and Jian Wang, Stanford University, were used as references for this section as similar measurement techniques are used.

If the light source is assumed to be monochromatic (the spectral width of the light source is much narrower than the absorption feature of interest), the Beer-Lambert relation is given as

$$T_\nu = \frac{I_{T,\nu}}{I_{0,\nu}} = \exp\left(-\int_0^L k_\nu(x)dx\right) \tag{1.1}$$

where T_ν is the transmission of a laser of frequency ν (cm-1), $I_{T,\nu}$ is the transmitted intensity, $I_{0,\nu}$ is the incident intensity, L is the path length, and k_ν is the spectral absorption coefficient. The spectral absorption coefficient of a media of N species with M_j contributing transitions is

$$k_\nu(x) = \sum_{j=1}^{N}\sum_{i=1}^{M_j} S_i(T)\phi_\nu(T,P,X_1,...,X_N)X_j P \tag{1.2}$$

where S_i is the linestrength and ϕ_ν is the lineshape function of transition *i* of species *j*, X_j is the mole fraction, and P is the total pressure.

The HITRAN database contains the spectroscopic constants of many IR-active species [1, 2]. Equation 1.3 is used to scale the linestrengths, given at a reference temperature, to other temperatures,

$$S_i(T) = S_i(T_0)\frac{Q(T_0)}{Q(T)}\left(\frac{T_0}{T}\right)\exp\left(\left[-\frac{hcE_i''}{k}\left(\frac{1}{T}-\frac{1}{T_0}\right)\right]\frac{1-\exp\left(\frac{-hc\nu_{0,i}}{kT}\right)}{1-\exp\left(\frac{-hc\nu_{0,i}}{kT_0}\right)}\right) \tag{1.3}$$

where E_i'' is the lower state energy level [1/cm] of the *i*th transition and *Q(T)* is the appropriate partition function, h is Planck's constant [J*s], c is the speed of light [cm/s], k is Boltzmann's constant [J/K]. The partition function, Q(T) is given in the HITRAN database.

Next, the lineshape, or broadening characteristics, of the transition must be approximated. At pressures near 1 atm, the Voigt profile is a good approximation to the lineshape function. The Voigt profile, resulting from a convolution of the Lorentzian (high-pressure) and Doppler (low-pressure) limits, is calculated as

$$\phi_\nu = \left(\frac{2\sqrt{\ln 2/\pi}}{\Delta\nu_D} \right) V\left[\frac{2\sqrt{\ln 2/\pi}}{\Delta\nu_D} \left(\nu - \nu_{0,i} - \Delta\nu_{,i} \right), a_i \right] \tag{1.4}$$

where *V()* is the Voigt function, $\Delta\nu_D$ is the Doppler width, and $\Delta\nu_s$ is the collision shift. Several algorithms for computing the Voigt function are available [3-5]. The parameter a_i is the relative weighting of the Doppler width and the collisional width

$$a_i = \sqrt{\ln 2}\,\frac{\Delta\nu_c}{\Delta\nu_D} \tag{1.5}$$

where $\Delta\nu_c$ is the collision width. The Doppler width is a function of the random motion of the absorbing molecules. Thus, the effect is the same on all molecules and results in a Gaussian profile as

$$\Delta\nu_D = 7.1623\times10^{-7}\sqrt{T/M} \tag{1.6}$$

where *M* is the molecular weight [amu] and *T* is the temperature [K]. The collision width, caused by dephasing effects of collisions, has varying effects on molecules and results in a Lorentzian profile as

$$\Delta\nu_c = P\sum X_j \delta_j^{\,T_0} \left(\frac{T_0}{T} \right)^{m_j} \tag{1.7}$$

where δ_j is the shift parameter and m_j is the temperature exponent. Although nearly an infinite number of transitions contribute to the absorption at each frequency, the wavelengths studied were chosen so that they are dominated by transitions of the species of interest. This is further discussed in Sections 3.1.1 and 3.2.1.

Linestrengths generally exhibit a much higher sensitivity to temperature than the lineshapes. Thus, the temperature in a media of unknown concentrations can be measured through a ratio of the absorption at two wavelengths. In a uniform media of a single absorbing species, the Beer-Lambert equation becomes, for two lasers,

$$T_\nu = \frac{I_{L,1}}{I_{0,1}} = \exp-\left(k_{\nu,1}L\right) = \exp\left(-S_1\phi_1 XPL\right) \tag{1.8}$$

$$T_\nu = \frac{I_{L,2}}{I_{0,2}} = \exp-\left(k_{\nu,2}L\right) = \exp\left(-S_2\phi_2 XPL\right)\ . \tag{1.9}$$

The ratio of the two spectral absorption coefficients is then

$$R_\nu = \frac{k_{\nu,1}}{k_{\nu,2}} = \frac{S_1\phi_1 XP}{S_2\phi_2 XP} = \frac{S_1\phi_1}{S_2\phi_2}. \tag{1.10}$$

If a single, isolated transition at low pressure is assumed, the spectral absorption coefficients can be integrated over the tuning range of the laser to remove the effects of the lineshape function and form the ratio R

$$R = \frac{K_1}{K_2} = \frac{S_1(T_0)\exp\left[\frac{-hcE_1"}{k}\left(\frac{1}{T}-\frac{1}{T_0}\right)\right]}{S_2(T_0)\exp\left[\frac{-hcE_2"}{k}\left(\frac{1}{T}-\frac{1}{T_0}\right)\right]} = \frac{S_1(T_0)}{S_2(T_0)}\exp\left[\frac{-hc}{k}(E_1"-E_2")\left(\frac{1}{T}-\frac{1}{T_0}\right)\right]. \tag{1.11}$$

Solving for the temperature

$$T = \frac{\frac{hc}{k}(E_2"-E_1")}{\ln\frac{K_1}{K_2} + \ln\frac{S_1(T_0)}{S_2(T_0)} + \frac{hc}{k}\frac{(E_2"-E_1")}{T_0}} \tag{1.12}$$

In reality, many transitions contribute to the temperature dependence. However, the temperature is dominated by the difference in lower state energies. Thus, the true relationship is solved for iteratively and then approximated by a simple function over a limited temperature range (see Section 3.1).

1.3.3 Chemiluminescence. Chemiluminescence occurs when an excited molecule, or radical, falls from an elevated energy state back to the ground state and emits light. Figure 1.2 illustrates the energy levels of a molecule. Each molecule emits radiation at

certain wavelengths. Thus, by choosing wavelengths where the radiation of the molecule of interest dominates, the intensity of radiation can be correlated to radical concentration.

.

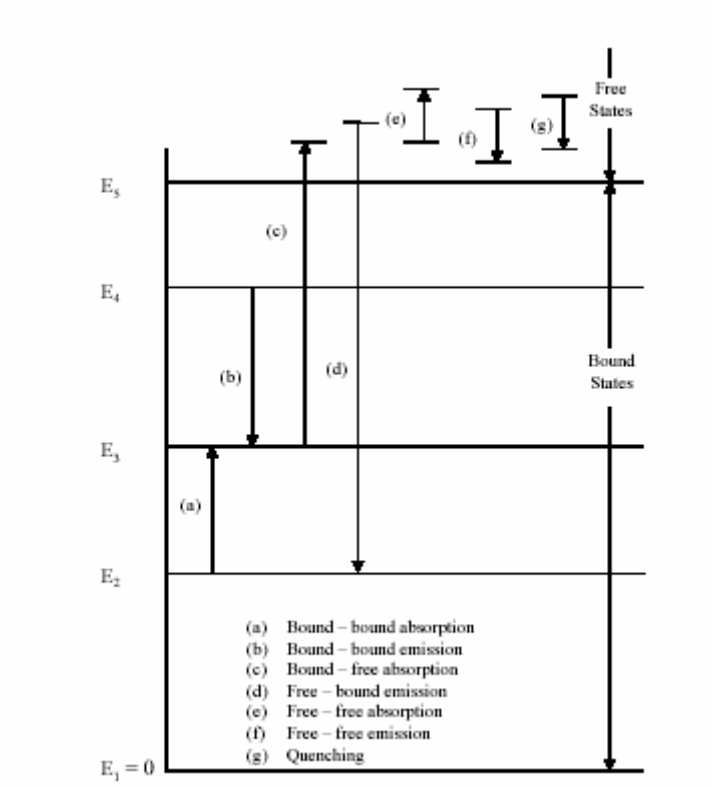

Figure 1.4. Energy Levels. Chemiluminescence results from an excited radial decreasing energy levels and emitting light [6].

In combustion, chemiluminescence measurements from the flame indicates there are far more radicals in the flame than predicted for equilibrium conditions at the flame temperature. Thus, the radicals must be a product of the chemical reactions taking place and should be a good indicator of the chemical reaction rate. In particular, hydroxyl radical (OH*) chemiluminescence has been used as an indicator of heat release rate in combustion systems. In this study, OH* chemiluminescence will be correlated to the chemical heat release rate of laminar and turbulent combustion systems.

1.3.4 Dynamic Systems. Dynamic systems are simply systems whose properties vary in time. It is often helpful to represent a dynamic system on an input/output basis. By using

equation 1.13, a series of differential equations in t can be transformed to a series of algebraic equations in s, assuming zero initial conditions,

$$\frac{d}{dt} = s \quad . \tag{1.13}$$

This transformation is called a Laplace Transform. The input/output relationship of a system, in terms of the Laplacian variable s, is known as a transfer function. The transfer function

$$G(s) = \frac{Y(s)}{U(s)} = \frac{(s+\alpha_1)(s+\alpha_2)...(s+\alpha_N)}{(s+\beta_1)(s+\beta_2)...(s+\beta_N)} \tag{1.14}$$

where *Y(s)* is the output, *U(s)* the input, the roots of the numerator are the zeros, and the roots of the denominator are the poles of the system. The poles determine the stability of the system. If a pole is greater than zero, the transient response will grow with time. If the poles of the system are less than zero, the transient response will decay.

The experimental representation of a transfer function is a frequency response function. To obtain a frequency response function, a linear system is forced at finite frequencies. The response of the output variable to the input is recorded at the forcing frequency. The result, over a range of frequencies, is called the frequency response function, or simply the frequency response. Analytical transfer functions can be fit to experimental frequency response functions.

Frequency response functions are complex quantities, i.e. consist of real and imaginary components. Frequency response functions are often plotted as magnitude and phase. A zero in the left half of the Laplace domain results in an increase in magnitude of 20dB/decade and a 90 degree rise in phase. A pole in the left half of the Laplace domain results in a decrease in magnitude of 20 dB/decade and a 90 degree drop in phase. Examples of common frequency response functions are shown in Figure 1.5.

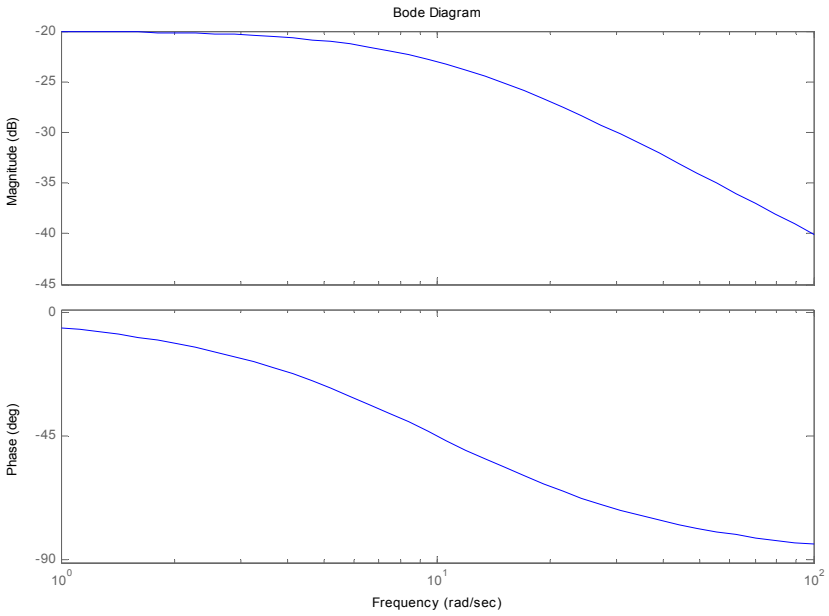

(a) real pole

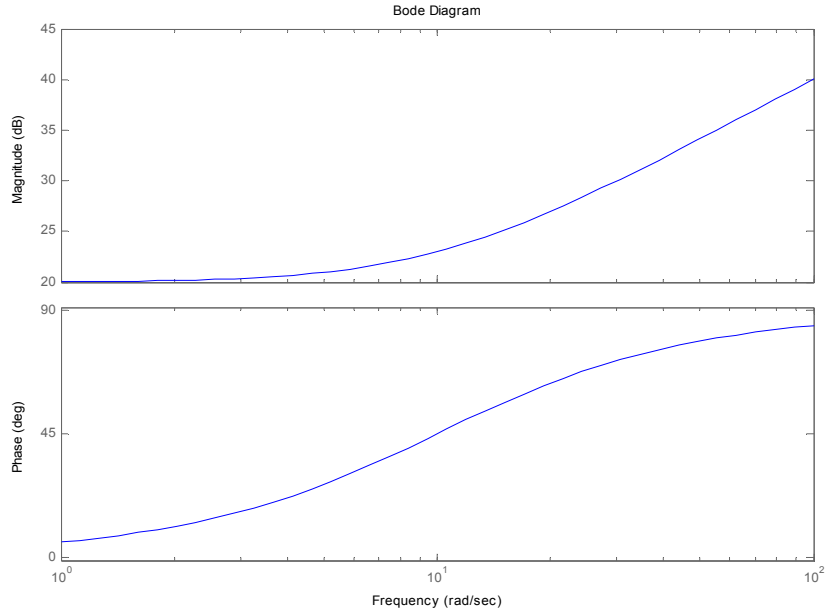

(b) real zero

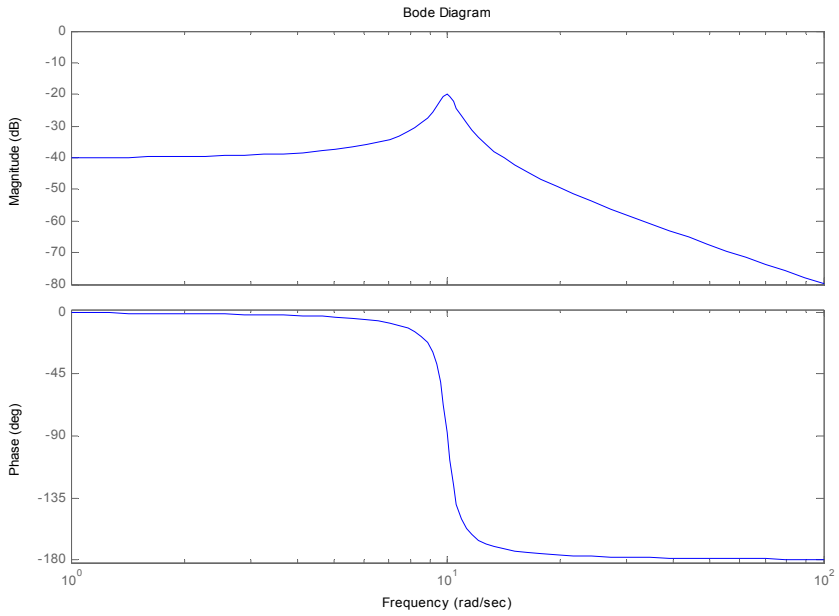

(c) complex-conjugate pair of poles

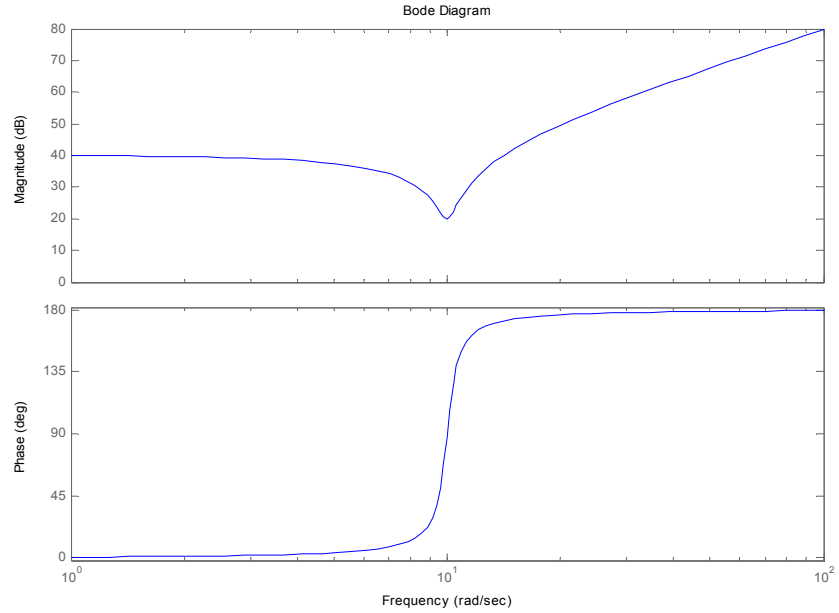

(d) complex-conjugate pair of zeros

Figure 1.5. Typical Frequency Response Functions. FRF's are often plotted as magnitude and phase.

Coherence is a measure of the extent to which there is a linear relationship between the input and output of a system. The coherence function is defined as

$$\gamma_{xy}^2(f) = \frac{\left|S_{xy}(f)\right|^2}{S_{xx}(f)S_{yy}(f)}$$

where S is the spectral density, x is the input, and y is the output. The coherence function ranges between 0 and 1, with a coherence of 1 indicating a perfectly linear relationship. Degradation of coherence can occur due to 1) extraneous noise in the measurement, 2) errors in the spectral density function estimates, 3) the output is a function of an input other than the input measured, and 4) nonlinearities [7].

Figure 1.1 is an example of a closed-loop system, i.e. feedback is present. No feedback is present in an open-loop system, as seen in Figure 1.6. In this study, we are striving for an open-loop model of the flame dynamics. The flame dynamics model can then be coupled with a model of acoustics in the feedback loop to simulate the closed-loop behavior of thermoacoustic instabilities.

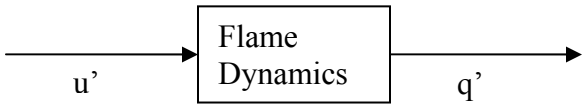

Figure 1.6. Open-Loop System. No feedback is present in an open-loop system.

1.3.5. Flame Dynamics. Flame dynamics are the time-varying effect of flow and chemical parameters on the heat release rate of a flame. Many factors influence flame dynamics. The mean flow rate and equivalence ratio affect the mean heat release rate as well as the dynamic heat release rate. Perturbations in these mean flow quantities, i.e. acoustics and equivalence ratio variations, cause an unsteady response. Large-scale, coherent hydrodynamic structures, such as vortices and shear layers, also affect the output of a flame. Combustion instabilities occur when the unsteady heat release rate feeds back into the flame via acoustics or equivalence ratio fluctuations, as seen in Figure 1.1. The instabilities grow until restrained by some nonlinear saturation effect, resulting in a limit cycle phenomenon. A limit cycle is characterized by sustained, self-excited

oscillations that are nearly sinusoidal. Combustion instabilities differ from pulsed combustion in that they are self-excited, and not forced. It is the objective of this study to develop models of flame dynamics in order to predict and control limit cycle phenomena.

1.4 Scope

The study presented here investigates the effect of perturbations in mass flow on the heat release rate in flames. Chemical heat release rate, or reaction rate, is measured via OH* chemiluminescence. The sensible heat release rate that feeds back into the acoustics, or the acoustic forcing function, is measured through product gas temperature. Two types of flames are studied: a laminar, flat-flame burner and a turbulent, swirl-stabilized combustor. Results are presented in transfer function form for a broad range of operating conditions.

The study is limited to the effect of acoustic perturbations on heat release rate. The effect of equivalence ratios is also integral to the problem and is left for future work. The current study attempts to measure *linear* flame dynamics. The true nature of unsteady combustion is a nonlinear process, thus linear models represent a large simplification. However, the linear dynamics are integral to the prediction of instabilities, as well as to the development of controllers. Knowledge of the linear dynamics will aid in understanding nonlinear dynamics. Atmospheric flames were studied while combustors in gas turbines often operate at several atmospheres of pressure. The scale of actual combustors is also much larger. Given the limitations, the flame dynamics observed in the study are expected to exhibit similar characteristics to combustors currently in use, as similar flame stabilization and mixtures are studied. The insight into the physics of flame dynamics will be applicable to full-scale gas turbines. More importantly, a methodology for measuring flame dynamics and developing dynamic models will be developed.

1.5 Approach

Using a systems level approach, the frequency–resolved response of unsteady heat release rate to perturbations in velocity is measured. Laser diagnostics are used to gain insight into the physical processes of combustion instabilities. Experiments are conducted on a turbulent, swirl-stabilized flame, much like combustors used in current gas turbines. Using the knowledge gained, low-order models of flame dynamics are be developed.

The methodology for developing models of flame dynamics is as follows:

1. Measure open-loop frequency response functions of flame dynamics by forcing acoustic perturbations and observing the effect in heat release rate.
2. Correlate governing dynamics with physical flame parameters.
3. Develop empirical flame transfer functions that describe the data.

By moving from simple to more complex flames, the effect of physical parameters can be observed separately. This "grassroots" approach ensures all of the relevant processes are included. Open-loop models of flame dynamics can then be coupled in a feedback loop with combustor acoustic models to predict TA instabilities.

To develop models of flame dynamics, one must measure the frequency response of the unsteady heat release rate that forces the acoustics, or the acoustic forcing function, to velocity perturbations. The acoustic forcing function is shown in equation 1.14, developed from the unsteady momentum, continuity, and energy equations [8].

$$\rho \cdot A \cdot c_p \cdot \frac{\partial T}{\partial t} + \dot{m} \cdot c_p \cdot \frac{\partial T}{\partial x} = Q_{force} \tag{1.14}$$

Recent numerical work [9] shows that OH* chemiluminescence is an excellent indicator of chemical reaction rate. However, OH* chemiluminescence does not indicate the dynamics of the acoustic forcing function well, as seen in Figure 1.7. The chemical heat release (CHR) and acoustic forcing function (Qforcing) coincide for low frequencies. At frequencies above 90 Hz, the convection begins to dominate the acoustic forcing function. Figure 1.8 shows that the acoustic forcing function is dominated by the $\partial T / \partial t$ term. Therefore, the unsteady temperature was used to measure acoustic forcing function dynamics using Tunable Diode Laser Absorption Spectroscopy (TDLAS). The

absorption of two water lines is recorded simultaneously to allow a dynamic measurement of gas temperature [10].

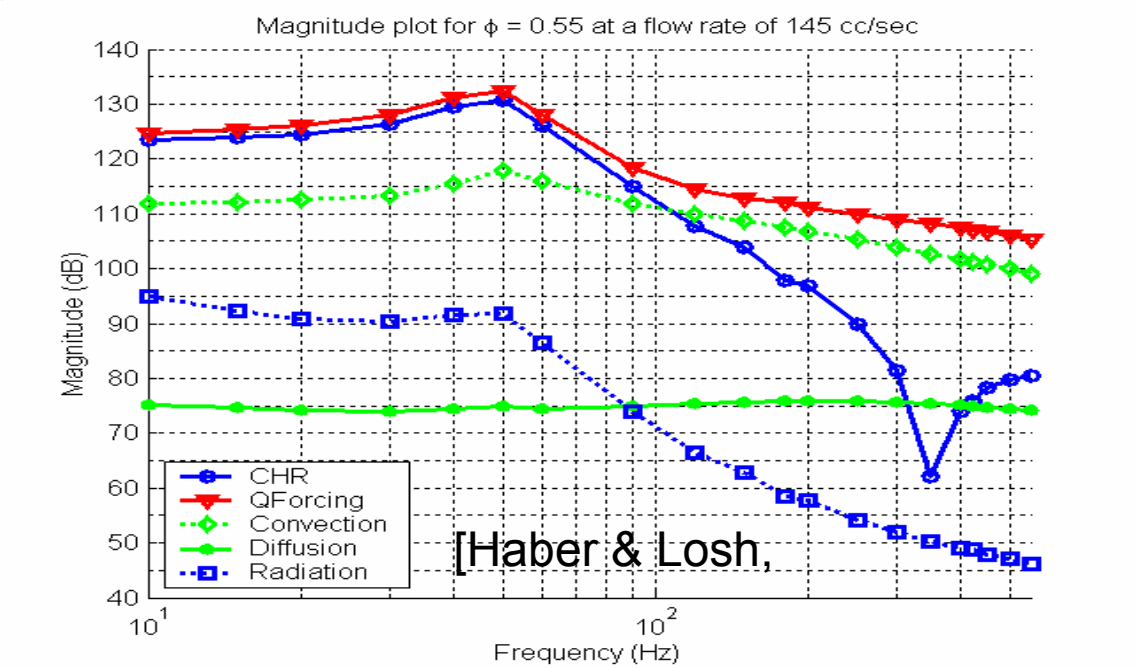

Figure 1.7. Frequency Response of Acoustic Forcing Term. A 1-D model including full chemistry and all modes of heat transfer was used [9].

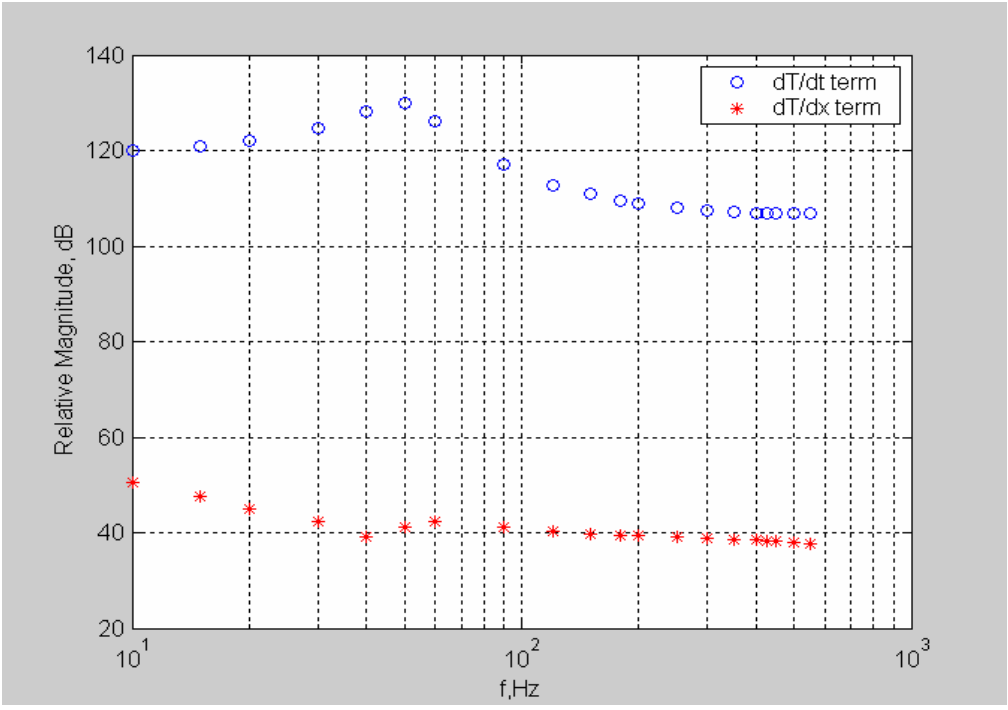

Figure 1.8. **Comparison of $\partial T / \partial t$ and $\partial T / \partial x$ Terms from 1-D Model.** The $\partial T / \partial t$ term dominates the acoustic forcing function.

The time lag of fluctuations in equivalence ratio is also important to stability. One coupling mechanism between acoustics and heat release rate is fluctuations in equivalence ratio, as seen in Figure 1.1. Equivalence ratio is defined as the air to fuel ratio over the stoichiometric air to fuel ratio. The time lag of interest is the time it takes for a perturbation in equivalence ratio to result in a fluctuation in heat release rate. To measure time lag, fluctuations in equivalence ratio will be observed upstream of the flame via methane absorption.

The chemical heat release rate is measured via OH* chemiluminescence. Through laser diagnostic techniques, sensible heat release rate, or acoustic forcing function, is measured. These measurements yield empirical flame transfer functions. Reduced-order models are based on the flame transfer functions. These compact models can then be used to predict combustor stability and implement active control techniques.

1.6 Structure of Thesis

The thesis describes the flame dynamics study and its results. Chapter Two reviews the relevant literature. The methods and procedures used in the experimental study are described in Chapter Three. Chapter Four discusses the results of the laminar flame dynamics study, and Chapter Five discusses the turbulent flame dynamics study. Chapter Six presents conclusions of the study and recommendations for further investigation.

Bibliography

1. Allen, M.G., *Diode laser absorption sensors for gas-dynamic and combustion flows.* Measurement Science Technology, 1998. **9**: p. 545-562.
2. Rothman, L.S. and e. al, *The HITRAN Molecular Spectroscopy Database and HAWKS (HITRAN Atmospheric Workstation): 1996 Edition.* Journal of Quantitative Spectroscopy and Radiative Transfer, 1998. **60**: p. 665-710.
3. Humlicek, J., *An efficient method for evaluation of the complex probability function: the Voigt function and its derivatives.* J. Quant. Spectrosc. Radiat. Transfer, 1979. **21**: p. 309-313.

4. Czosnyka, T., Trzcinska, A., *Unified analytical approximation of Gaussian and Voigtian lineshapes.* Nuclear Instruments and Methods in Physics Research, 1999. **A 431**: p. 548-550.
5. Rocco, H.O., D.I. Iriarte, and J. Pomarico, *General expression for the Voigt function that is of special interest for applied spectroscopy.* Society for Applied Spectroscopy, 2001. **55**(7): p. 822-826.
6. Khanna, V., *A study of the dynamics of laminar and turbulent fully and partially premixed flames*, in *Mechanical Engineering*. 2001, Virginia Tech: Blacksburg, VA.
7. Bendat, J.S., *Nonlinear System Analysis and Identification from Random Data*. 1990.
8. Annaswamy, A.M. and A.F. Ghoniem, *Active control in combustion systems.* IEEE Controls Systems, 1995: p. 49-63.
9. Haber, L. and U. Vandsburger. *Combustion and heat transfer dynamics in a premixed laminar flat-flame burner*. in *Aerospace Sciences Meeting*. 2004.
10. Furlong, E.R., *Diode-laser absorption spectroscopy applied for the active control of combustion*, in *Mechanical Engineering*. 1998, Stanford University: Stanford, CA.